

ESO VLT optical spectroscopy of BL Lacertae objects. III. An extension of the sample.

B. Sbarufatti

*INAF, Istituto di Astrofisica Spaziale e Fisica Cosmica di Palermo
Via Ugo La Malfa 153, I-90146 Palermo, Italy
sbarufatti@ifc.inaf.it*

S. Ciprini

*1. Physics Department University of Perugia, and I.N.F.N. Perugia Section,
Via A. Pascoli, I-06123 Perugia, Italy
2. Tuorla Observatory, University of Turku,
Väisäläntie 20, FIN-21500 Piikkiö, Finland*

J. Kotilainen

*Tuorla Observatory, University of Turku
Väisäläntie 20, FIN-21500 Piikkiö, Finland*

R. Decarli, A. Treves, A. Veronesi

*Università dell'Insubria
Via Valleggio 11, I-22100 Como, Italy
and*

R. Falomo

*INAF, Osservatorio Astronomico di Padova
Vicolo dell'Osservatorio 5, I-35122 Padova, Italy*

ABSTRACT

We present results of an ongoing program at the ESO VLT for spectroscopy of BL Lac objects lacking a firm redshift estimate and here we report on 15 objects. For 11 sources we confirm the BL Lac classification, and we determine new redshifts for 3 objects, 1 with weak emission lines (PKS 1057–79, $z = 0.569$) and 2 with absorptions from the host galaxy (RBS 1752, $z = 0.449$; RBS 1915, $z = 0.243$); moreover a sub Damped Lyman Alpha (sub-DLA) system is detected in the direction of the BL Lac PKS 0823–223 ($z \geq 0.911$). For the remaining 8 BL Lacs, from the very absence of absorption lines of the host galaxy, lower limits to the redshift are deduced with z_{\min} in the interval 0.20 – 0.80. The remaining three sources are reclassified as a FSRQ (PKS 1145–676, $z = 0.210$; TXS 2346+052, $z = 0.419$) and a misclassified galactic star (PMNJ 1323–3652).

Subject headings: BL Lacertae objects: general

1. Introduction

Blazars dominate the scene of extragalactic gamma ray astronomy as space borne missions and Čerenkov atmospheric telescopes have shown. BL Lac objects (BL Lacs or BLLs) are a main sub-class of *blazars* that by definition exhibit featureless spectra or very weak lines, most probably because of the relativistic enhancement of the continuum. Surely, the recent launch of AGILE and GLAST gamma-ray observatories and the upgrading of the existing ground-based Čerenkov telescopes will significantly increase the interest in the BL Lac objects. The determination of the redshift is mandatory in order to characterize these sources (e.g. to determine nuclear and host galaxy luminosity of the sources), but it is arduous, in most of the objects, to detect the weak spectral features over the continuum. Indeed, a redshift determination exists for only about half of the known BLLs. The detection of the weak spectral lines necessarily requires the use of 8–10 meters telescopes. In addition to the issue of redshift, high S/N and spectral resolution are also of importance for detecting the host galaxy independently of imaging, since its emission may appear superposed to the non-thermal continuum of the nucleus. Absorption lines may be related to the host galaxy itself, to the intergalactic medium and to the interstellar medium of our galaxy and its halo. The emission lines are the most direct probe to the physical conditions around the nucleus.

We have an ongoing program for BL Lac’s spectroscopy at the European Southern Observatory (ESO) 8–meter Very Large Telescope (VLT), which utilizes the telescope in service mode under non-optimal seeing conditions. The results of the first three runs (2003 and 2004) referred to 35 BLLs. We measured new redshifts for 17 sources, while for the rest of the objects we have given upper limits using a technique specifically designed for this project. Details are given in Sbarufatti et al. (2005b, 2006b, S05 and S06 in the following), together with the criteria on the sample selection.

In this paper we present the spectra of 15 objects observed in 2006 (Guest Observer run: ESO 077.B-0045). Data reduction and analysis procedures are described in section 2. Results are reported in section 3 along with specific comments about each source. Summary and conclusion are given in section 4. Throughout this paper we assume the following cosmological parameters: $H_0=70 \text{ km s}^{-1} \text{ Mpc}^{-1}$, $\Omega_\Lambda=0.7$, $\Omega_m=0.3$.

2. Observations and data analysis

The observations (Table 1) were performed between 2006 March through August in Service Mode at the ESO VLT UT2 (Kueyen) telescope, equipped with the FOcal Reducer and low dispersion Spectrograph (FORS1), using the 300V+I grism combined with a $2''$ slit, yielding a dispersion of 112 Å mm^{-1} (corresponding to $2.64 \text{ Å pixel}^{-1}$) and a spectral resolution of 15 Å covering the 3800–8000 Å range. The seeing during observations was in the range 0.5–2.5'', with an average of 1''.

We performed data reduction using IRAF¹ (Tody 1986, 1993), following the standard procedures for spectral analysis. This includes bias subtraction, flat fielding, and removal of bad pixels. For each target, we obtained three spectra for an optimal correction of the cosmic rays and to check for the reality of weak spectral features. The individual frames were then combined into a single average image. Wavelength calibration was performed using the spectra of a He/Ne/Ar lamp, resulting in an accuracy of $\sim 3 \text{ Å}$ (rms). From these calibrated final images, we extracted the one-dimensional spectra inside a $2'' \times 6''$ aperture, adopting an optimal extraction algorithm (Horne 1986) to improve the Signal to Noise ratio (S/N).

As a part of a fill-in program, our observations did not require optimal photometric conditions. However, the sky was clear for most of the observations. This enabled us to perform a spectrophotometric calibration of the data using standard stars (Oke 1990). We estimate an uncertainty of the order of 10% in the flux calibration because of the not optimal sky condition. Flux losses due to the slit not being oriented along the parallactic angle are negligible with respect to the flux calibration uncertainties. All the spectra were dereddened following the extinction law by Cardelli et al. (1989) and assuming the E_{B-V} values computed by Schlegel et al. (1998).

3. Results

In Figure 1 we give the optical spectrum for each source. In order to make apparent the shape of the continuum and the faint spectral features, we report both the flux calibrated and the normalized spectra.

¹IRAF (Image Reduction and Analysis Facility) is distributed by the National Optical Astronomy Observatories, which are operated by the Association of Universities for Research in Astronomy, Inc., under cooperative agreement with the National Science Foundation.

Intrinsic and intervening spectral features are identified with atomic species. Absorptions caused by the Galactic interstellar medium are indicated with ISM for simple atomic species, and with DIB (Diffuse Interstellar Band) for complex molecules. The Earth symbol is used to mark telluric absorptions. All spectra can be retrieved in electronic form at <http://www.oapd.inaf.it/zblac/>, where all the results of our program are archived.

3.1. Continuum emission and host galaxy contribution

The optical spectrum of a BL Lac can be described, in a first approximation, as the superposition of two components. The first one is a non-thermal continuum emitted by the active nucleus. The second is the contribution from the stars and the ISM of the BLL host galaxy. Extensive studies in the past (e.g. Urry et al. 2000) have shown that these galaxies are usually giant ellipticals the optical magnitudes of which follow a narrow Gaussian distribution centered around $M_R^{\text{host}} = -22.9 \pm 0.5$ (Sbarufatti et al. 2005a). In most cases the host galaxy signature was not detected in our spectrum because it was too faint with respect to the nuclear component. For these objects, we performed a fit of the optical continuum with a simple power-law model ($F_\lambda \propto \lambda^{-\alpha}$). In two cases however (RBS 1752 and RBS 1915) the host galaxy spectral features were detected, and we performed a fit to the spectrum using a two component model (see Fig. 2): a power-law plus an elliptical galaxy spectrum as in the template given in Kinney et al. (1996, see also S06 for details on the fitting procedure). The results from our fits are reported in Table 2, where for each object we give the power-law index, the object class (High Energy Peaked BLL, HBL; Low Energy Peaked BLL, LBL, see Padovani & Giommi 1995, for a definition) the apparent magnitude, and the extinction coefficient. For RBS 1752 and RBS 1915 we report also the absolute magnitudes of the host galaxies corrected for the aperture effect which were $M_R = -23.3$ and $M_R = -22.4$ respectively, in agreement with the expected distribution.

3.2. Line detection and redshift determination

Since emission and absorption lines in a BLL spectrum can be very faint, their detection can be a difficult task. Using the same technique presented in S06, we estimated the minimum detectable equivalent

width EW_{min} for each spectrum, and considered all features with equivalent width (EW) above this threshold as line candidates which were then carefully inspected for identification or rejection. EW_{min} values for each spectrum are given in table 1, while line identifications, Full Width Half Maximum (FWHM) and EW are reported in table 3. The continuum and line properties confirmed the BL Lac classification for 12 objects. In section 3.3 we report notes on the individual sources.

3.2.1. Redshift lower limits

Most of the confirmed BLL in our sample show featureless spectra, despite the high S/N reached using VLT. As extensively discussed in S06 (4.2.4), it is possible to estimate a lower limit to the redshift of such sources, knowing the EW_{min} and the nucleus apparent magnitude and exploiting the assumption that BL Lac hosts can be considered as candles (Sbarufatti et al. 2005a). We remark here that Equation 1 in S06 contains a typographical error, which was noted also by Finke et al. (2008). The correct expression is:

$$EW_{\text{obs}} = \frac{(1+z) \times EW_0}{1 + \rho/A(z)} \quad (1)$$

where EW_{obs} is the observed equivalent width, EW_0 is the equivalent width of the feature in the host galaxy template (Kinney et al. 1996), ρ is the nucleus-to-host flux ratio, z is the redshift and $A(z)$ is the aperture correction.

We applied this procedure to all featureless spectra in the sample, obtaining the lower limits reported in section 3.3.

3.3. Notes on individual objects.

PKS 0019+058 This radio selected source (Condon & Jauncey 1974) was first classified as a BLL by Fricke et al. (1983), based on a featureless optical spectrum. We observed this object in two epochs separated by about a month, noticing an optical variability of 0.7 mag (R band) and an evolution of the spectral index from 0.65 to 0.76. The reality of the optical variability is fully confirmed by the R -band images exposed prior to the spectra which enable direct photometry. The optical variability was known, both in magnitude ($V = 19.2$ and $V > 21$ in Fricke et al. 1983; Abraham et al. 1991, respectively) and in spectral index ($\alpha_v = 0.8$ and 0.94 in Fricke et al. 1983; Chen et al. 2005). We find no intrinsic feature with $EW > EW_{\text{min}}$ in any of the two

spectra. The NaI λ 5891 absorption from the Galaxy ISM is detected in both spectra with $EW = 0.43$ Å (July 12) and 0.66 Å (August 8). A marginally significant excess around 5600 Å is present in both observations, but it is most probably spurious because of a residuals left after the subtraction of a nearby atmospheric emission line. The most stringent redshift lower limits, obtained from the August 2006 spectrum is $z > 0.64$.

GC 0109+224 This source was discovered in radio observations by Davis (1971), and subsequently classified as a BL Lac by Owen & Muffson (1977). Strong flux and polarization variability was reported both in the radio and optical band (e.g. Katajainen et al. 2000; Ciprini et al. 2003, 2004). Optical imaging by Falomo (1996) and Nilsson et al. (2003) failed to detect the host galaxy, while the detection reported by Wright et al. (1998) is dubious, since it has not been confirmed by any subsequent observation. The lower limit on the redshift proposed by Falomo (1996) is $z > 0.4$. Previous optical spectroscopy by Wills & Wills (1979); Falomo et al. (1994); Sbarufatti et al. (2006a) performed with 2–4 m class telescopes showed featureless spectra, while Healey et al. (2008) report $z=0.265$ for this object based on an unpublished optical spectrum. The lower limit to the redshift as deduced by Sbarufatti et al. (2006a) was based on an $EW_{\min} = 0.43$ Å that yielded $z > 0.18$. The considerably higher S/N spectrum we obtained with VLT has $EW_{\min} = 0.09$ Å, which in turn implies $z > 0.25$, which improves the previous spectroscopical limit, but it is still less stringent than the imaging limit.

RBS 0231 This X-ray-selected object (Voges et al. 1999) was classified as a BLL by Schwöpe et al. (2000), and as a HBL by Brinkmann et al. (2000). No previous optical spectroscopy was published. The VLT spectrum is featureless, with $EW_{\min} = 1.27$ Å, which implies $z > 0.41$.

PKS 0823–223 This radio selected BL Lac (Allen et al. 1982) is characterized by a number of absorption lines in the UV and optical band (e.g. Rao & Turnshek 2000; Meiring et al. 2007; Falomo 1990; Veron et al. 1990; Falomo et al. 1994). These features are consistent with the presence of a sub-Damped Lyman α Absorber at $z = 0.91$. In our VLT spectrum we detect the absorption features of FeII λ 2373.7, 2383.2,

2585.9, 2599.4, MgII λ 2798 and MgI λ 2852 at the same redshift.

PKS 1057–79 This radio selected object (Shimmins & Bolton 1981) was proposed as a counterpart for the γ -ray source 2EGS 1050–7650 by Tornikoski et al. (2002). No previous optical spectroscopy was published. Our VLT spectrum shows several emission lines ([OIII] λ 4959,5007, [NeIII] λ 3868, MgII λ 2798), at $z = 0.581$. Since the FWHM of the MgII line (see table 3) is in excess of 1000 km s^{-1} we propose to classify this object as a broad line AGN.

PKS 1145–676 This radio source was classified as a quasar due to its point-like appearance by White et al. (1987). The flat radio spectrum and optical variability (Beasley et al. 1997; Costa 2002) prompted a *blazar* classification. We detect several emission lines ([OIII] λ 3727, H β λ 4861, [OIII] λ 4959,5007, H α λ 6563, [NII] λ 6585) at $z = 0.210$. The observed EW are in the range 4–25 Å, pointing towards a FSRQ classification. The FWHM of the H β line could indicate that this source is a narrow lines object, but the fact that we are unable to measure the H α FWHM due to the blending with the [NII] lines permits only a type ~ 1.9 classification.

OM 280 This radio selected source (Colla et al. 1972) was classified as a BLL due to its featureless spectrum by Strittmatter et al. (1974). Subsequent optical spectroscopy by Rector & Stocke (2001) also failed to discover any intrinsic spectral feature. The host galaxy was not detected in deep HST imaging (Urry et al. 2000), implying $z > 0.63$ (Sbarufatti et al. 2005a). The VLT spectrum is featureless, with $EW_{\min} = 0.35$ Å, which implies a redshift lower limit of 0.20, less stringent than the one from imaging.

PMN J1323–3652 This radio selected source was classified as a candidate BL Lac by the WGA catalog (White et al. 2000) and the Deep X-ray Radio Blazar survey (DXRBS, Landt et al. 2001), that also provided a featureless optical spectrum. However, our VLT optical spectrum clearly shows the absorption lines and the characteristic shape of a Galactic F-type star. This indicates a mis-identification of the optical counterpart of this source.

OQ 012 This radio selected BLL (Weiler & Johnston 1980) showed a featureless optical spectrum in observations by Falomo et al. (1994). Richards et al. (2004) gave a photometric redshift estimate $z = 0.475$ based on data from the Sloan Digital Sky Survey (SDSS). Our VLT spectrum shows an absorption line by Galactic ISM (NaI $\lambda 5891$), but no intrinsic features. The EW_{\min} is 0.31 \AA , which implies $z > 0.65$, inconsistent with the photometric estimate.

PMNJ 1539–0658 This radio source (Griffith et al. 1995) was classified as a BL Lac in the DXRBS (Landt et al. 2001), which also provided a featureless optical spectrum. In the VLT spectrum we detect the NaI $\lambda 5891$ absorption line from the Galaxy, but no intrinsic features. The minimum detectable EW is 0.61 \AA , which implies $z > 0.80$.

PKS 1830–589 This radio-selected BL Lac (Griffith et al. 1995; Landt et al. 2001) showed a featureless optical spectrum when observed in the DXRBS. Our VLT spectrum is also featureless (NaI $\lambda 5891$ is marginally detected with $EW = 0.4 \text{ \AA}$). The minimum detectable equivalent width is $EW_{\min} = 0.46 \text{ \AA}$, which gives a lower limit $z > 0.45$.

RBS 1752 This X-ray-selected BLL (Voges et al. 1999) had a tentative redshift $z = 0.449$ proposed in the Sedentary Survey (Giommi et al. 2005a; Piranomonte et al. 2007), based on the possible detection of the host galaxy spectral features in an ESO 3.6 m optical spectrum. The high S/N obtained using VLT allowed us to detect some weak host galaxy lines (CaII $\lambda 3934, 3968$, G band $\lambda 4305$, and MgI $\lambda 5175$) at $z = 0.449$. However, the G band is possibly contaminated by the [OI] atmospheric line at 6300 \AA , and the MgI line is very close to the telluric O_2 A band. therefore, while the absorption features reported by Piranomonte et al. (2007) are confirmed, the redshift remains tentative because of the lack of other firm absorption features. The fit to the spectrum with a power-law plus elliptical galaxy model gives $M_R^{\text{host}} = -23.3$, in good agreement with the expected distribution $M_R^{\text{host}} = -22.9 \pm 0.5$.

RBS 1915 This X-ray selected object (Voges et al. 1999) was classified as a BLL by Schwobe et al. (2000). The optical spectrum reported by Chavushyan et al. (2000) was featureless. Our VLT spectrum shows

faint absorption lines from the BLL host galaxy (CaII $\lambda 3934, 3968$, G band $\lambda 4305$, and MgI $\lambda 5175$) at $z = 0.243$. We performed a fit to the spectrum using a power-law plus elliptical galaxy model, obtaining $M_R^{\text{host}} = -22.4$, consistent with the expected distribution ($M_R^{\text{host}} = -22.9 \pm 0.5$).

TXS 2346+052 This radio selected source (Large et al. 1981) was classified as a BL Lac because of its flat radio spectrum (Gorshkov et al. 2000) and the featureless optical spectrum (Chavushyan et al. 2000). Our VLT spectrum shows several emission lines (MgII $\lambda 2798$, [OII] $\lambda 3727$, [NeIII] $\lambda 3868$, [OIII] $\lambda 4959, 5007$) at $z = 0.419$. The observed EW of the MgII and [OIII] lines (exceeding 5 \AA), rules out a BL Lac classification and suggests a FSRQ nature for this source. The EW ratio between the [OII] and [OIII] lines are untypical for an AGN, possibly indicating an ongoing star formation (as seen in PKS 2005–489 by Bressan et al. 2006). A measurement of the equivalent width of the $H\alpha + [\text{NII}]$ line system (which is out of the observed spectral range) could help to clarify this issue.

1RXS J235730.1–171801 This X-ray selected object (Voges et al. 1999) was classified as a BLL by Schwobe et al. (2000). Our previous VLT observations (S06) gave a limit $z > 0.85$. The spectrum presented here has a slightly lower S/N (110, to be compared with 150 of the earlier observation, because of the different seeing conditions between the observations), that gives $EW_{\min} = 0.22 \text{ \AA}$ and $z > 0.60$. CaII $\lambda 3934$ and NaI $\lambda 5891$ absorptions from the Galaxy ISM are marginally detected (they were also detected in the S06 spectrum, along with several DIBs). No significant flux variations were detected between two different observation periods.

4. Summary and conclusions

Of 15 observed objects, we confirm the BL Lac classification for 11 sources, and the detection of a sub-DLA system in PKS 0823–223 ($z \geq 0.911$). PKS 1145–676 and TXS2346+052 are reclassified as FSRQ ($z = 0.210$ and $z = 0.419$ respectively), while PMN J1323–3652 is a F-type star. For 4 BLLs we are able to give a new determination of the redshift (PKS 1057–79 $z = 0.569$; RBS 1752 $z = 0.448$; RBS 1915, $z = 0.243$). For the remaining 8 BLLs, we give redshift lower limits based on the minimum detectable

equivalent width of their featureless spectra. On the whole, our BL Lac spectroscopy database now contains 45 confirmed BL Lacs observed with VLT, with 20 redshifts determined by detection of faint lines, and 25 redshift lower limits.

In those cases where even VLT+FORs observations are inconclusive, a further increase in the S/N ratio is required, for example through the use of adaptive optics, Very Large Telescope Interferometry, the Large Binocular Telescope, observations in the near infrared region, where the nucleus-to-host ratio is smaller than in the optical range, or, in the future, even the use of Extremely Large Telescopes. Alternatively, it would be possible to observe these sources when the active nucleus goes into a low state, since the decrease in the N/H ratio would make easier to detect the features of the host galaxy.

Based on observations collected at the European Organisation for Astronomical Research in the Southern Hemisphere, Chile. Observing proposal: ESO 077.B-0045 (PI: S. Ciprini). SC acknowledges the funding by the European Community's Human Potential Programme under contract HPRN-CT-2002-00321.

REFERENCES

- Abraham, R. G., Crawford, C. S., & McHardy, I. M. 1991, *MNRAS*, 252, 482
- Allen, D. A., Ward, M. J., & Hyland, A. R. 1982, *MNRAS*, 199, 969
- Bauer, F. E., Condon, J. J., Thuan, T. X., & Broderick, J. J. 2000, *VizieR Online Data Catalog*, 212, 90547
- Beasley, A. J., Conway, J. E., Booth, R. S., Nyman, L.-A., & Holdaway, M. 1997, *A&AS*, 124, 469
- Bressan, A., Falomo, R., Valdés, J. R., & Rampazzo, R. 2006, *ApJ*, 645, L101
- Brinkmann, W., Laurent-Muehleisen, S. A., Voges, W., et al. 2000, *A&A*, 356, 445
- Cardelli, J. A., Clayton, G. C., & Mathis, J. S. 1989, *ApJ*, 345, 245
- Chavushyan, V., Mujica, R., Gorshkov, A. G., Konnikova, V. K., & Mingaliev, M. G. 2000, *Astronomy Letters*, 26, 339
- Chen, P. S., Fu, H. W., & Gao, Y. F. 2005, *New Astronomy*, 11, 27
- Ciprini, S., Tosti, G., Raiteri, C. M., et al. 2003, *A&A*, 400, 487
- Ciprini, S., Tosti, G., Teräsranta, H., & Aller, H. D. 2004, *MNRAS*, 348, 1379
- Colla, G., Fanti, C., Fanti, R., et al. 1972, *A&AS*, 7, 1
- Condon, J. J. & Jauncey, D. L. 1974, *AJ*, 79, 1220
- Costa, E. 2002, *A&A*, 381, 13
- Davis, M. M. 1971, *AJ*, 76, 980
- della Ceca, R., Palumbo, G. G. C., Persic, M., et al. 1990, *ApJS*, 72, 471
- Donato, D., Ghisellini, G., Tagliaferri, G., & Fossati, G. 2001, *A&A*, 375, 739
- Edwards, P. G. & Tingay, S. J. 2004, *A&A*, 424, 91
- Falomo, R. 1990, *ApJ*, 353, 114
- Falomo, R. 1996, *MNRAS*, 283, 241
- Falomo, R., Scarpa, R., & Bersanelli, M. 1994, *ApJS*, 93, 125
- Finke, J. D., Shields, J. C., Böttcher, M., & Basu, S. 2008, *A&A*, 477, 513
- Flesch, E. & Hardcastle, M. J. 2004, *A&A*, 427, 387
- Fricke, K. J., Kollatschny, W., & Witzel, A. 1983, *A&A*, 117, 60
- Ghosh, K. K. & Soundararajaperumal, S. 1995, *ApJS*, 100, 37
- Giommi, P., Piranomonte, S., Perri, M., & Padovani, P. 2005a, *A&A*, 434, 385
- Giommi, P., Piranomonte, S., Perri, M., & Padovani, P. 2005b, *VizieR Online Data Catalog*, 343, 40385
- Gorshkov, A. G., Konnikova, V. K., & Mingaliev, M. G. 2000, *Astronomy Reports*, 44, 353
- Griffith, M. R., Wright, A. E., Burke, B. F., & Ekers, R. D. 1995, *ApJS*, 97, 347
- Healey, S. E., Romani, R. W., Cotter, G., et al. 2008, *ApJS*, 175, 97

- Horne, K. 1986, *PASP*, 98, 609
- Katajainen, S., Takalo, L. O., Sillanpää, A., et al. 2000, *A&AS*, 143, 357
- Kinney, A. L., Calzetti, D., Bohlin, R. C., et al. 1996, *ApJ*, 467, 38
- Landt, H., Padovani, P., Perlman, E. S., et al. 2001, *MNRAS*, 323, 757
- Large, M. I., Mills, B. Y., Little, A. G., Crawford, D. F., & Sutton, J. M. 1981, *MNRAS*, 194, 693
- Meiring, J. D., Lauroesch, J. T., Kulkarni, V. P., et al. 2007, *MNRAS*, 376, 557
- Nass, P., Bade, N., Kollgaard, R. I., et al. 1996, *A&A*, 309, 419
- Nieppola, E., Tornikoski, M., & Valtaoja, E. 2006, *A&A*, 445, 441
- Nilsson, K., Pursimo, T., Heidt, J., et al. 2003, *A&A*, 400, 95
- Oke, J. B. 1990, *AJ*, 99, 1621
- Owen, F. N. & Muffson, S. L. 1977, *AJ*, 82, 776
- Padovani, P. & Giommi, P. 1995, *ApJ*, 444, 567
- Piranomonte, S., Perri, M., Giommi, P., Landt, H., & Padovani, P. 2007, *A&A*, 470, 787
- Rao, S. M. & Turnshek, D. A. 2000, *ApJS*, 130, 1
- Rector, T. A. & Stocke, J. T. 2001, *AJ*, 122, 565
- Richards, G. T., Nichol, R. C., Gray, A. G., et al. 2004, *ApJS*, 155, 257
- Sbarufatti, B., Falomo, R., Treves, A., & Kotilainen, J. 2006a, *A&A*, 457, 35
- Sbarufatti, B., Treves, A., & Falomo, R. 2005a, *ApJ*, 635, 173
- Sbarufatti, B., Treves, A., Falomo, R., et al. 2005b, *AJ*, 129, 559
- Sbarufatti, B., Treves, A., Falomo, R., et al. 2006b, *AJ*, 132, 1
- Schlegel, D. J., Finkbeiner, D. P., & Davis, M. 1998, *ApJ*, 500, 525
- Schwöpe, A., Hasinger, G., Lehmann, I., et al. 2000, *Astronomische Nachrichten*, 321, 1
- Shimmings, A. J. & Bolton, J. G. 1981, *Australian Journal of Physics*, 34, 471
- Strittmatter, P. A., Carswell, R. F., Gilbert, G., & Burbidge, E. M. 1974, *ApJ*, 190, 509
- Tody, D. 1986, in Presented at the Society of Photo-Optical Instrumentation Engineers (SPIE) Conference, Vol. 627, Instrumentation in astronomy VI; Proceedings of the Meeting, Tucson, AZ, Mar. 4-8, 1986. Part 2 (A87-36376 15-35). Bellingham, WA, Society of Photo-Optical Instrumentation Engineers, 1986, p. 733., ed. D. L. Crawford, 733–+
- Tody, D. 1993, in Astronomical Society of the Pacific Conference Series, Vol. 52, Astronomical Data Analysis Software and Systems II, ed. R. J. Hanisch, R. J. V. Brissenden, & J. Barnes, 173–+
- Tornikoski, M., Lähteenmäki, A., Lainela, M., & Valtaoja, E. 2002, *ApJ*, 579, 136
- Urry, C. M., Scarpa, R., O’Dowd, M., et al. 2000, *ApJ*, 532, 816
- Veron, P., Veron-Cetty, M.-P., Djorgovski, S., et al. 1990, *A&AS*, 86, 543
- Voges, W., Aschenbach, B., Boller, T., et al. 1999, *A&A*, 349, 389
- Vollmer, B., Davoust, E., Dubois, P., et al. 2005, *A&A*, 431, 1177
- Weiler, K. W. & Johnston, K. J. 1980, *MNRAS*, 190, 269
- White, G. L. 1992, Proceedings of the Astronomical Society of Australia, 10, 140
- White, G. L., Batty, M. J., Bunton, J. D., Brown, D. R., & Corben, J. B. 1987, *MNRAS*, 227, 705
- White, N. E., Giommi, P., & Angelini, L. 2000, *VizieR Online Data Catalog*, 9031, 0
- Wills, B. J. & Wills, D. 1979, *ApJS*, 41, 689
- Wright, S. C., McHardy, I. M., Abraham, R. G., & Crawford, C. S. 1998, *MNRAS*, 296, 961
- Wu, Z., Jiang, D. R., Gu, M., & Liu, Y. 2007, *A&A*, 466, 63

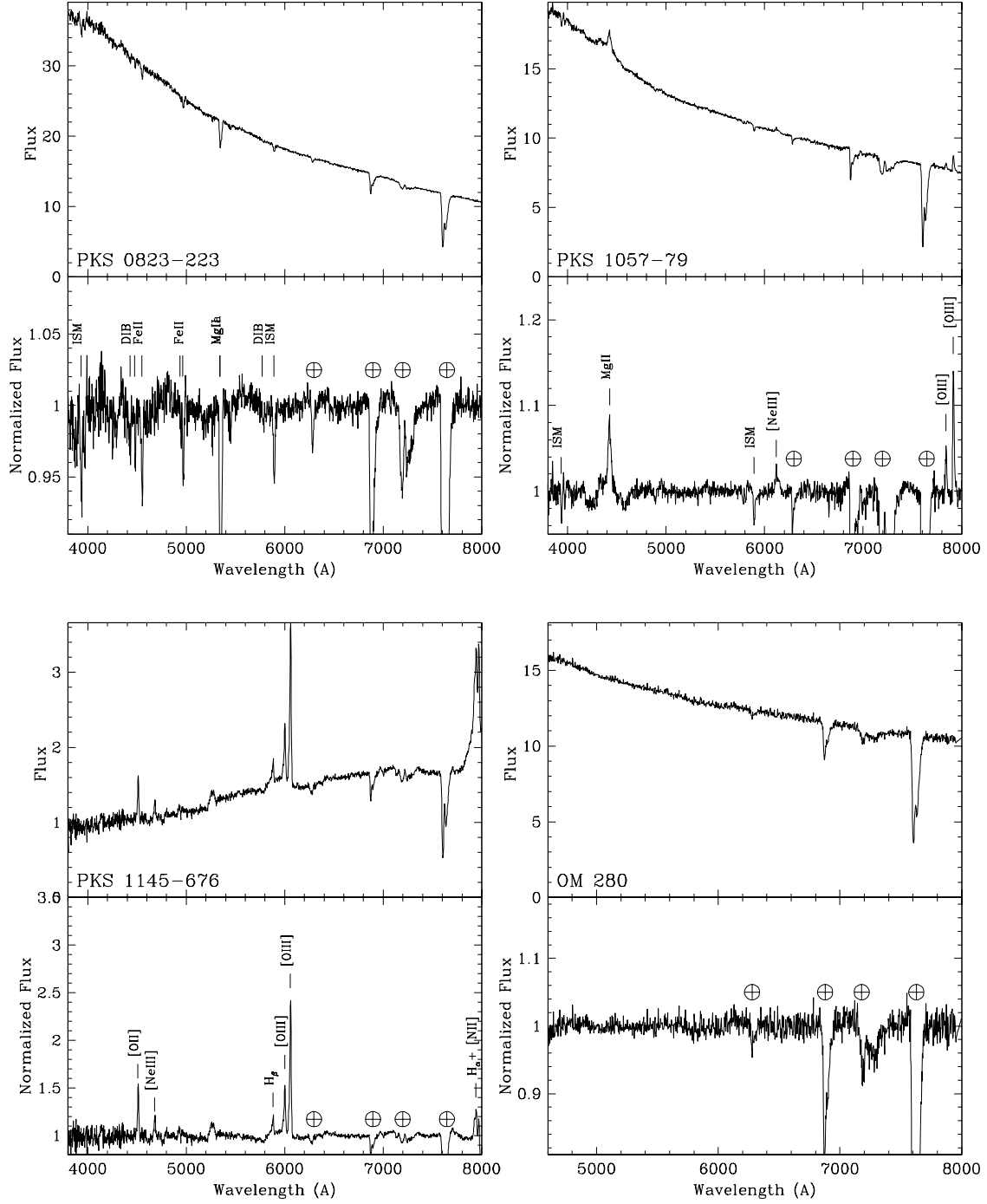


Fig. 1.— continued

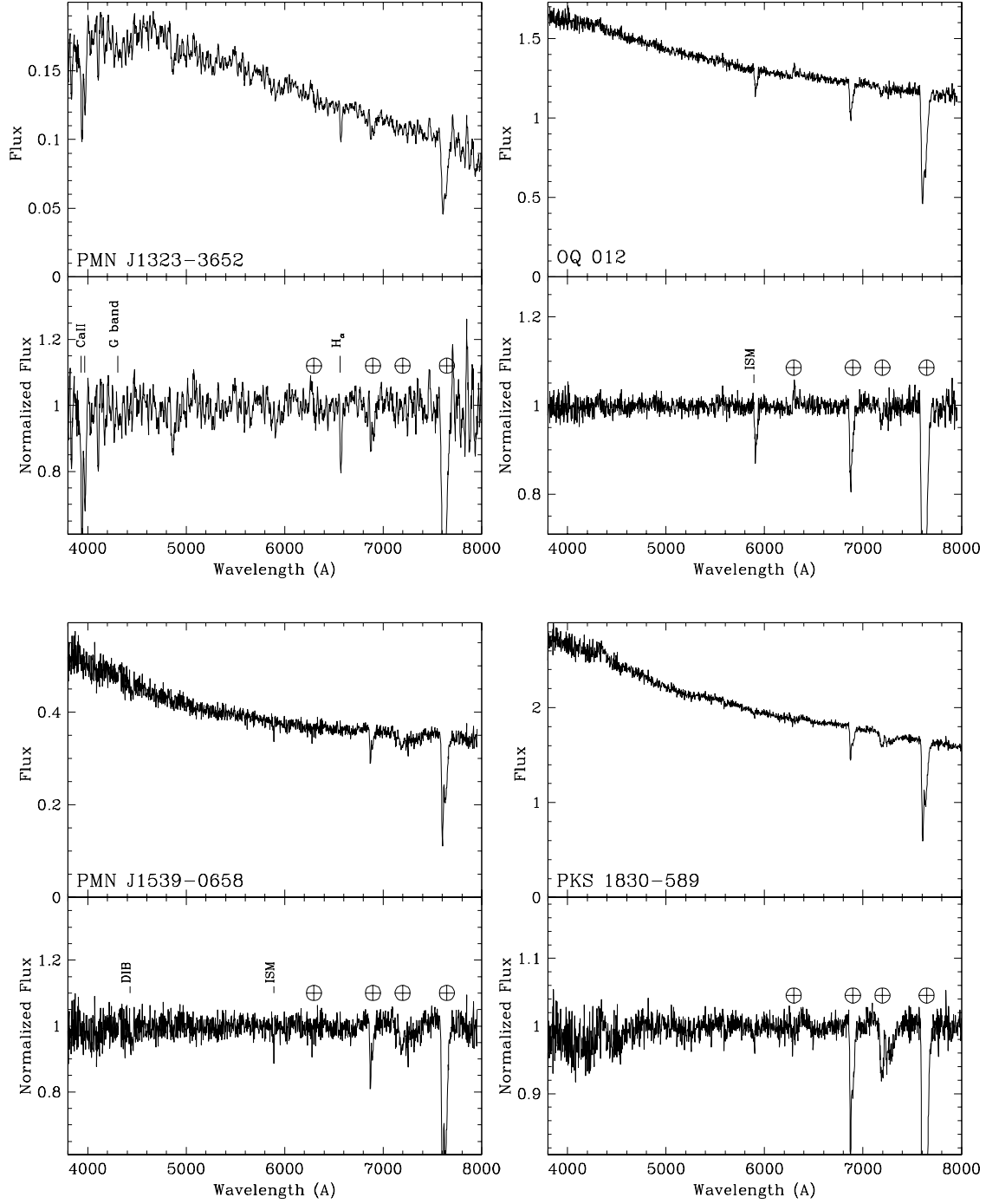


Fig. 1.— continued

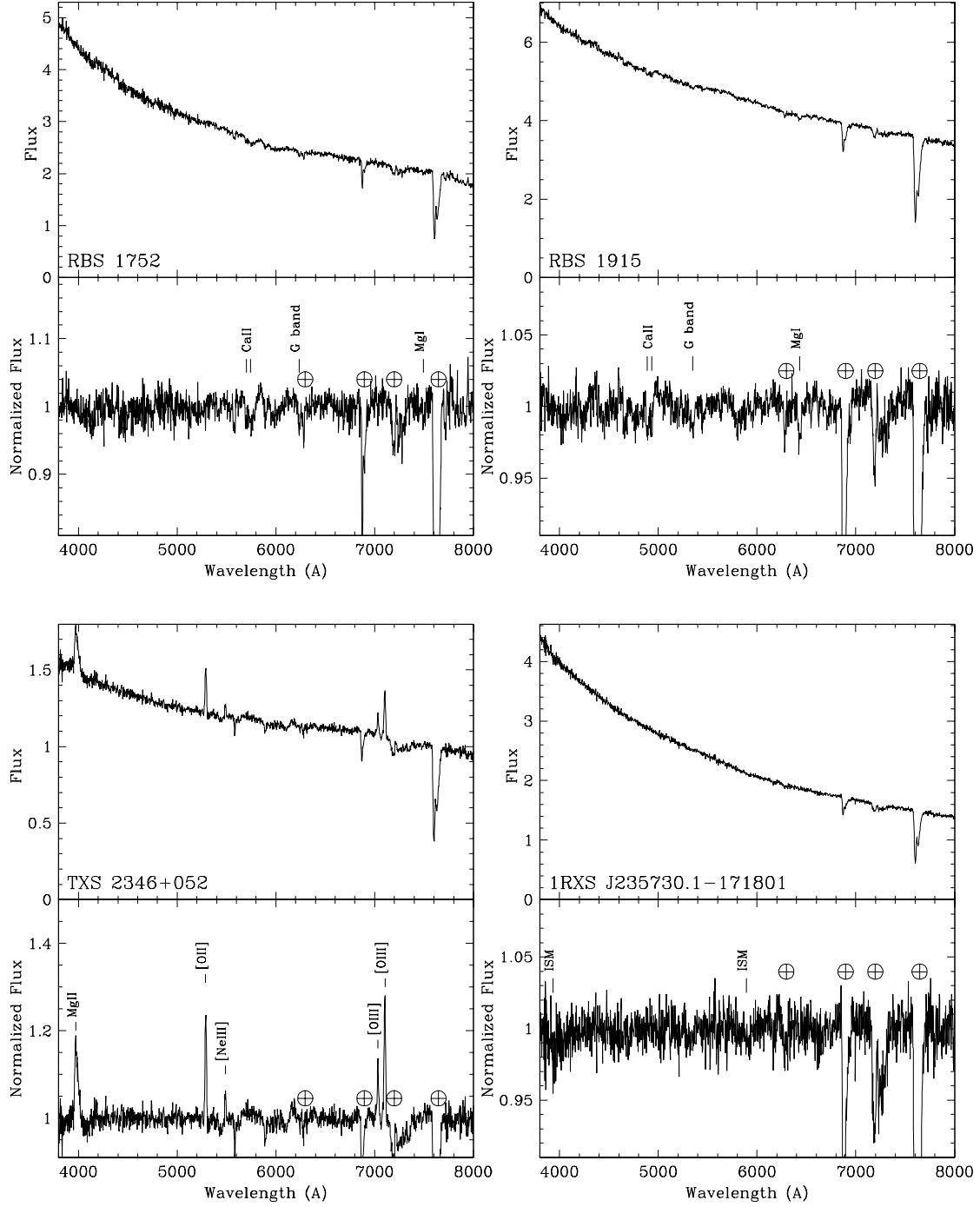


Fig. 1.— continued

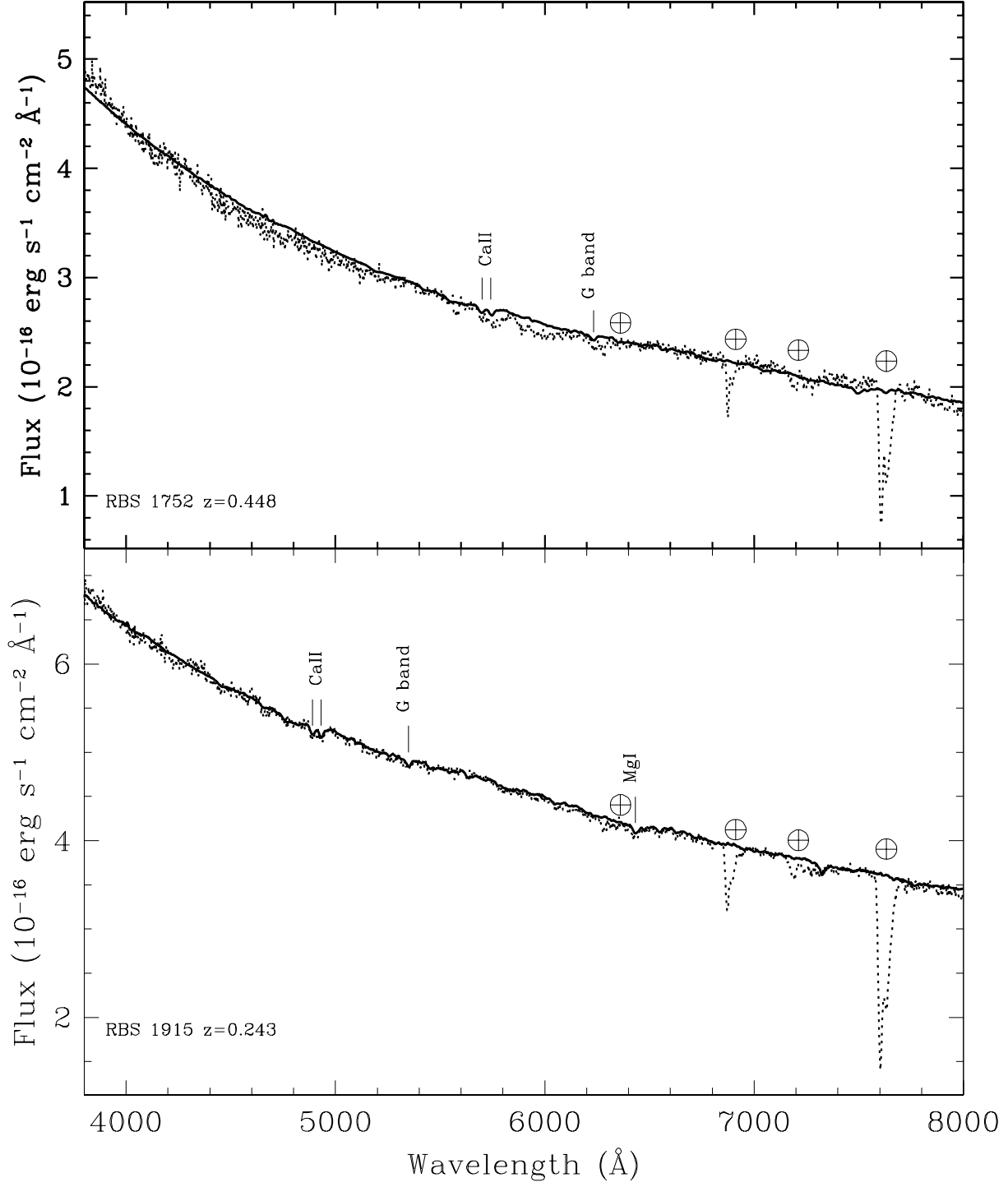


Fig. 2.— Spectral decomposition for objects RBS 1752 and RBS 1915. Solid line shows the fitted spectrum, dotted line the observed one.

TABLE 1
JOURNAL OF OBSERVATIONS

Object name	IAU name	RA (J2000)	Dec (J2000)	Date of obs.	Exposure s	S/N	EW _{min} Å	z
(1)	(2)	(3)	(4)	(5)	(6)	(7)	(8)	(9)
PKS 0019+058	0019+058	00 22 32	+06 08 04	Jul 12	2400	120	0.38	>0.49
...	Aug 08	2400	70	0.40	>0.64
GC 0109+224	0109+224	01 12 06	+22 44 39	Sep 01	4065	380	0.09	>0.25
RBS 0231	none	01 40 41	−07 58 49	Jul 13	2400	20	1.27	>0.41
PKS 0823−223	0823-223	08 26 02	−22 30 27	Apr 14	2400	220	0.41	≥0.911
PKS 1057−79	1057-797	10 58 43	−80 03 54	Mar 31	2400	90	0.39	0.581
PKS 1145−676	1145-676	11 47 33	−67 53 42	Apr 14	2400	80	1.84	0.210
OM 280	1147+245	11 50 19	+24 17 54	Apr 16	2400	100	0.35	>0.20
PMN J1323−3652	none	13 23 46	−36 53 39	May 07	2400	20	1.57	0
OQ 012	1407+022	14 10 04	+02 03 07	May 07	2400	120	0.31	>0.63
PMNJ 1539−0658	none	15 39 10	−06 58 43	Mar 28, Apr 20	4800	50	0.61	>0.80
PKS 1830−589	1830-589	18 34 28	−58 56 36	Apr 15	2400	100	0.46	>0.45
RBS 1752	none	21 31 35	−09 15 23	May 10	2400	90	0.49	0.448
RBS 1915	none	22 56 13	−33 03 38	May 05	2400	160	0.35	0.243
TXS 2346+052	2346+052	23 49 21	+05 34 40	Jul 01	2400	80	0.63	0.419
1RXS J235730.1−171801	none	23 57 30	−17 18 05	Jul 01	2400	110	0.22	>0.63

NOTE.—Description of columns: (1) Object name; (2) IAU J1950 code-name; (3) Right Ascension (J2000); (4) Declination (J2000); (5) Date of observations, year 2006; (6) Exposure time; (7) Signal to Noise; (8) Minimum detectable EW, calculated following Sbarufatti et al. (2006b); (9) Redshifts measured from spectral features and redshift lower limits.

TABLE 2
SPECTRAL FITS

Object name (1)	α (2)	M_R^{host} (3)	Class (4)	R (5)	E(B-V) (6)	(7)
PKS 0019+058	-0.65		L	17.7	0.023	N96,G00
PKS 0019+058	-0.76		L	18.4	0.023	N96,G00
GC 0109+224	-0.82		L	14.6	0.049	N96,W07
RBS 0231	-1.00		L	18.6	0.109	G05
PKS 0823-223	-0.47		H	15.4	0.472	D90,W92
PKS 1057-79	-0.73		L	15.9	0.306	F04,E04
OM 280	-0.79		L	15.7	0.027	D01,G95
OQ 012	-0.29		L	18.1	0.108	N06
PMNJ 1539-0658	-0.50		L	19.5	0.156	L01
PKS 1830-589	-0.65		L	17.7	0.095	L01
RBS 1752	-1.45	-23.3	L	17.5	0.037	G05
RBS 1915	-1.09	-22.4	L	16.8	0.018	B00
TXS 2346+052	-0.06		L ¹	18.3	0.187	V05
1RXS J235730.1-171801	-1.40		H	17.7	0.070	G05

NOTE.—(1) Object name; (2) Spectral index of the continuum, α , defined by $F_\lambda \propto \lambda^{-\alpha}$; (3) absolute R magnitude of the host galaxy; (4) Class of the object (H: High energy peaked BL Lac, L: Low energy peaked BL Lac); (5) apparent R magnitude of the object, extracted within a 6''x2'' aperture; (6) Galactic extinction in the direction of the object, from Schlegel et al. (1998). (7) References for HBL/LBL classification: D90: della Ceca et al. (1990), W92: White (1992), G95: Ghosh & Soundararajaperumal (1995), N96: Nass et al. (1996), B00: Bauer et al. (2000), G00: Gorshkov et al. (2000), D01: Donato et al. (2001), L01: Landt et al. (2001), E04: Edwards & Tingay (2004), F04:Flesch & Hardcastle (2004), G05: Giommi et al. (2005b), V05: Vollmer et al. (2005), N06: Nieppola et al. (2006), W07: Wu et al. (2007).

¹Source lacking an X-ray detection in literature. The LBL classification is tentative.

TABLE 3
SPECTRAL LINES.

Object name	Object Class	z	Line ID	Wavelength \AA	z_{line}	Type	FWHM km s^{-1}	EW \AA
(1)	(2)	(3)	(4)	(5)	(6)	(7)	(8)	(9)
PKS 0823–223	sub-DLA/BLL	≥ 0.911	Galactic CaII K	3935	0	i	1700	1.85
			Galactic CaII H	3970	0	i	1500	1.00
			FeII	4481	0.911	a	800	0.47
			FeII	4553	0.911	a	1300	1.33
			FeII	4948	0.914	a	600	0.30
			FeII	4970	0.912	a	800	0.85
			MgII	5349	0.911	a	1300	4.12
			MgI	5452	0.911	a	600	0.44
			Galactic NaI	5893	0	i	900	1.08
PKS 1057–79	BLL	0.581	MgII	4423	0.581	e	3400	-4.24
			NeIII	6119	0.582	e	300	-0.25
			[OIII]	7842	0.581	e	500	-1.25
			[OIII]	7917	0.581	e	500	-3.58
PKS 1145–676	QSO	0.210	[OII]	4512	0.210	e	1000	9.25
			[NeIII]	4680	0.210	e	1200	3.99
			H β	5880	0.210	e	900	5.52
			[OIII]	6001	0.210	e	1000	9.14
			[OIII]	6059	0.210	e	800	24.66
			H α	7944	0.210	e
			NII	7970	0.210	e
RBS 1752	BLL	0.448	CaII	5693	0.447	g	1000	0.5
			CaII	5749	0.449	g	1900	0.9
			G band	6237	0.449	g	1200	1.0
			MgI	7493	0.448	g	600	0.4
RBS 1915	BLL	0.243	CaII	4890	0.243	g	1700	0.75
			CaII	4932	0.243	g	1100	0.46
			G band	5351	0.243	g	2600	0.88
			MgI	6429	0.243	g	1900	1.96
TXS 2346+052	FSRQ	0.419	MgII	3973	0.420	e	3600	-7.0
			[OII]	5290	0.419	e	1000	-5.0
			[NeV]	5488	0.419	e	800	-1.2
			[OIII]	7033	0.418	e	700	-2.1
			[OIII]	7103	0.419	e	700	-5.3

NOTE.—Description of columns: (1) Object name; (2) Object class; (3) average redshift; (4) line identification; (5) observed wavelength of line center; (6) redshift of the line; (7) type of the line (e: emission line, g: absorption line from the host galaxy, a: absorption line from intervening systems), i: absorption line from our Galaxy ISM); (8) FWHM of the line; (9) EW of the line;